Heliyon 10 (2024) e33680

Contents lists available at ScienceDirect

Heliyon

journal homepage: www.cell.com/heliyon

Research article

Experimental and drying kinetics study on millet particles by a pulsating fluidized bed dryer

Milad Setareh [a,*], Mohammad Reza Assari [a,b], Hassan Basirat Tabrizi [c], Alireza Maghamian Zadeh [a]

[a] *Mechanical Engineering Department, Jundi-Shapur University of Technology, Dezful, Iran*
[b] *Department of Mechanical Engineering, Faculty of Engineering, Alzahra University, Tehran, Iran*
[c] *Mechanical Engineering Department, Amirkabir University of Technology, Tehran, Iran*

ARTICLE INFO

Keywords:
Drying
Foxtail millet
Fluidized bed
Pulsating flow
Semi-empirical models

ABSTRACT

This research studies experimentally the drying of foxtail millet in a pulsation-assisted fluidized bed. The effects of temperature and pulsating flow frequency on millet drying are examined. The experiments are conducted at temperatures of 40 °C, 50 °C, and 60 °C for three pulsating frequencies of 0.5, 1, and 2.5 Hz and continuous flow. The best result is obtained for drying with a frequency of 1 Hz. It shows that the pulsating flow is more effective at 50 °C as compared to other temperatures. Four reliable semi-empirical models are used for predicting the moisture reduction during drying process. Among the fitted dynamic models, the model that has the maximum correlation coefficient (R^2) and minimum sum of squares of error (*SSE*) and root mean squared error (*RMSE*) and well able to predict the behavior of millet drying in the whole process was chosen.

1. Introduction

Millet is a traditional food, which is cultivated widely in Eurasian regions with mild climates. It is also the sixth most important grain in the world. Millet is considered a suitable food source for developing countries and has advantages such as a short crop season, resistance to dryness, storage capability, and high adaptability. It contains many nutrients and can be used in a balanced diet [1]. Millets are mostly consumed as a major ingredient in traditional foods, such as puree and bread. Furthermore, they are a rich source of vegetable proteins, leucine, aspartic acid, alanine, phenylalanine, valine, proline, and lysine. Researchers have shown an increased interest in vegetable proteins due to the increase in the cost of animal proteins. The global demand for food-based proteins is expected to increase by more than one-third of the present demand with a twofold increase in population by 2050 [2].

All agricultural products have a moisture content when harvested. This moisture level increases the risk of attacks by fungi, pests, and microbes and the growth of microorganisms. It may also result in damage to or discoloration of the grains. For example, the annual grain loss in China due to insufficient drying and microbial spoilage has reached 21 million tons [3]. The storage time of millet decreases significantly with an increase in moisture. In general, the moisture content below 10 % is considered safe for long-term storage [4].

In recent years, numerous studies have been carried out on grain drying and new drying techniques have been developed. Several of

* Corresponding author. Mechanical Engineering, Jundi-Shapur University of Technology, Dezful, P. O. Box 64615/334, Iran.
E-mail address: msetare@jsu.ac.ir (M. Setareh).

https://doi.org/10.1016/j.heliyon.2024.e33680
Received 12 March 2024; Received in revised form 23 May 2024; Accepted 25 June 2024
Available online 26 June 2024
2405-8440/

these techniques are introduced as convective hot air drying, heat pump drying, microwave drying, solar drying, fluidized bed drying, infrared drying, and hybrid drying [5–7]. Among various hot air drying techniques, fluidized bed drying (FBD) is a novel method capable of drying food continuously and in large quantities with uniform moisture removal, less drying time, high drying speed, and without over-drying [8,9]. Fluidized beds are known due to better mixing of particles, which is required for achieving a uniform drying quality in terms of moisture and diameter distribution [10,11]. The drying speed in a fluidized bed can be affected by various factors, such as operational conditions, bed geometry, and grain properties such as size, initial moisture, and density [12].

Pulsating fluidization is a special case of fluidized beds where the gas flow velocity varies periodically with time. Pulsation improves particle mixing by reducing the mixing time and resulting in more homogeneous mixtures as compared to continuous flows. Nabipoor Hassankiadeh et al. [13] showed that the pulsation not only shortens the drying time but enhances uniformity during drying of particles. Pulsation prevents the agglomeration of wet particles, enhances the mixing behavior of materials, and reduces channeling and bypassing. Moreover, they showed the effect of the pulsation frequency of 1.0–2.0 Hz on the fluidized bed drying of potash particles.

The frequency of the pulsed flow is a critical factor that can affect the fluidization behavior. Gas-solid flow behavior in a pulsed fluidized bed was studied experimentally and numerically by Khosravi Bizhaem and Basirat Tabrizi [14]. They looked to the effect of pulsating flow with a frequency range of 1–10 Hz for particle sizes of Geldart B and A/B group with variation of particle density. Further, they indicated that at low pulse frequencies, large bubbles would form and move upward, increasing the bed expansion ratio and pressure fluctuation. A rise in the pulse frequency decreases the bubble size, bed expansion ratio, and pressure fluctuation. Using solenoid valves is the most common way to generate pulsating flows; the frequency, amplitude, waveform, and fluid flow rate are the main parameters in a pulsating flow [15]. The pulsating flow entering the pulsed fluidized bed dryer (PFBD) can improve the system performance by good mixing, uniformity of particles and better gas-particle contact [16,17].

The fluidized bed drying has been successfully used to dry agricultural products such as biomass particles, cumin, corn, beans, peas, soybean, apple, mint leaves, rice, etc. [18]. Liu et al. [19] empirically investigated the fluidization of high-moisture particles of various sizes in pulsating flows. They demonstrated that the combination of pulsating and continuous flows accelerates particle mixing. Nabipoor Hassankiadeh et al. [20] studied experimentally the impact of pulsation frequency, mass flow rate ratio and initial relative humidity on the drying process of potash particles in a pulsed fluidized bed. They concluded that the drying process becomes optimum with the pulsation frequency, and mass flow rate ratio of 1 Hz and 0.33, respectively. Jia et al. [21] investigated the effect of pulsed frequency between 0.75 and 6 Hz on the drying of biomass particles. Their results indicated that increasing the pulsation frequency converts the system state from periodic fluidization at 0.75 and 1.5 Hz to apparently steady fluidization at 3 and 6 Hz. In addition, the highest heat transfer coefficients among different frequencies were seen between 1 and 1.5 Hz. Bengtsson et al. [22] investigated the effect of air temperature and flow velocity on the total drying time of sawdust experimentally. They showed that the air velocity had a smaller influence as compared to the air temperature on the constant-rate drying period. Khanali et al. [23] studied experimentally the drying process of rough rice in a fluidized bed. They found that the minimum total energy is obtained for an air temperature of 70 °C and superficial fluidization velocity of 2.3 m/s.

In a drying process, the simultaneous investigation of heat and mass transfer is known to be complex. Therefore, it is difficult to develop a mathematical model to predict the dependent variables in terms of the independent variables in this process. Although numerous methods have been developed for predicting drying kinetics, most of these methods have low accuracy in predicting moisture drop during drying. The most common method for the prediction of moisture removal is experimental or regression modeling. The drying kinetics is an important indicator for confirming the optimality of the process parameters [24,25]. In a study on moisture removal from papaya seeds to prevent microbial activity, Alhanif et al. [26] examined the effect of the drying temperature on the characteristics of the effective moisture ratio (*MR*) graph and fitted the experimental *MR* to a semi-empirical model. Three models were used to predict the *MR* of papaya seeds, and the logarithmic model was considered the most suitable one for determining the *MR* in drying papaya seeds. Sozzi et al. [27] used a fluidized bed to dry blackberry waste. A semi-empirical model was employed to fit the drying data, and a sufficiently accurate relationship was obtained.

As stated, using FBDs can be useful in several ways:

- Helping to fluidize particles that have higher viscosity and are difficult to fluidize
- Preventing or reducing particle agglomeration and eliminating inactive regions, which is an effective technique for modifying gas particle contact and, hence, improving bed efficiency.
- Increasing the heat and mass transfer rate between fluidized beds and fixed surfaces and between the gas passing over the bed and the particles in the bed.

Studying the literature shows that at a given gas velocity, an optimized increase in the pulsating frequency can improve mixing, increase the heat transfer coefficient in the bed, and enhance the drying rate. Nevertheless, an excessive increase or decrease in the pulsating frequency reduces heat transfer and drying performance [28]. However, the effect of pulsed fluidization on heat transfer via the fluidized bed has not been fully understood although it has been a topic of interest to researchers in recent years. There have been limited studies on the influence of heat transfer with gas pulsation in fluidized beds [29].

This study looks to the experimental drying of foxtail millet grains for pulsating frequency in the fluidized bed at 0.5–2.5 Hz. This is new for this particular grain and shows what kind of model can be used for this process. The effect of changing the inlet flow condition from steady to pulsating and varying the frequency are investigated. The influence of changes in the inlet air temperature as an important factor affecting moisture removal is also studied. Besides, the moisture removal process is represented by a semi-empirical model in order to predict this drying process.

2. Materials and methods

2.1. Setup and experimental procedure

An experimental apparatus of a pulsed fluidized bed dryer is constructed and the experiments of drying of foxtail millet grains are carried out as shown in Fig. 1. The setup is made of a plexiglass tube with an internal diameter of 0.145 m and a height of 1 m, and a fine grid screen with a 14 % free surface is placed at the bottom to separate the solid particles in the fluidized bed from the air inlet chamber. In general, published information on the engineering properties of foxtail millet is limited, although there is consistency between various authors in the properties that have been studied and the hydration behavior of grains is still under investigation. Originally, the water absorption capacity of foxtail millet is around 1.90 and water solubility index is 2.8 % [30]. In this study, the foxtail millet used for the tests and the physical and chemical specifications are shown in Table 1 [30,31]. The moisture content of the used grains was 0.1 % on a dry basis. After spraying 10 g of water per 90 g and then being placed in a refrigerator for 24 h to gain moisture absorption, its humidity was brought to 0.234 % on a dry basis. By this method, the humidity ratio reaches a value so that the particles do not dry quickly in the experiments. The millet samples with a diameter of 2.50 ± 0.1 mm are separated via gradation, and 500 g of the prepared product is poured into the bed in each test.

The compressed air flow is supplied by piston compressors and converted to a pulsed flow by using a solenoid valve to generate the airflow with a square waveform. The airflow is heated up by passing through a heater and finally is entered the bed. In order to measure the changes in the moisture content with time, a 10 g millet sample is extracted from the bed at specific intervals and kept in closed containers. After being weighed, the samples are placed in an oven at a temperature of 105 °C.

In order to determine the optimal drying conditions and the effect of the pulsed flow compared to the continuous flow, the tests are conducted at different temperatures of 40 °C, 50 °C, and 60 °C for pulsation frequencies of 0.5, 1, and 2.5 Hz and the continuous flow. In order to repeatability removing the effect of possible errors, each experiment is carried out three times and the average of obtained

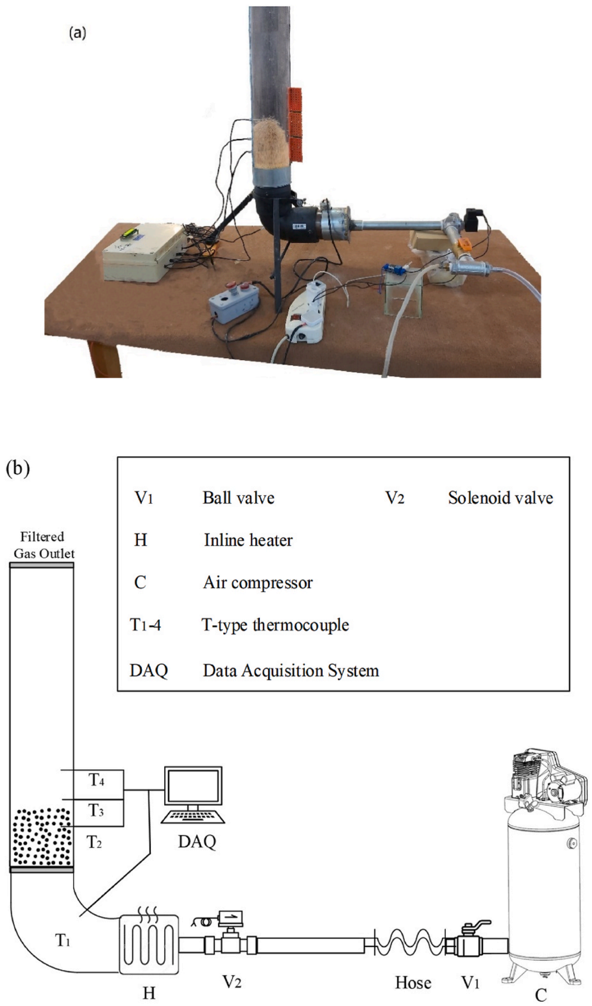

Fig. 1. Pulsed fluidized bed dryer setup. (a) Picture of apparatus, (b) Schematic view.

Table 1
Properties of the Foxtail millet per 100 g [30,31].

Physical property	Value	Chemical property	Value
True density (kg/m^3)	1264.82 ± 1.02	Protein (g)	12.3
Apparent density (kg/m^3)	735.70 ± 0.50	Carbohydrate (g)	60.9
Porosity (%)	41.08 ± 1.0	Fat (g)	4.3
Angle of repose (°)	25.78 ± 0.04	Fiber (g)	8
Diameter (10^{-3} m)	2.50 ± 0.1	Minerals (g)	3.3
Water solubility index	2.8 %	Metabolizable energy (kcal)	351

results is presented. The weight reduction in the samples during drying is measured using a digital scale at specific intervals until the moisture ratio (*MR*) difference between the samples reaches below 0.02 % on a dry basis. The conditions and parameters of experiments are written in Table 2.

2.2. Minimum fluidization velocity

In a normal fluidized bed, the cavity is filled with bed materials up to a specific height, known as the bed height. As the inlet gas velocity increases up to the minimum fluidization velocity (U_{mf}), the stationary bed begins to fluidize. The increase in velocity creates a bubble bed and leads to the pneumatic displacement of particles, where the whole bed is fully fluidized [32]. The velocity of air entering the bed is calculated by air mass flow rate divided by the cross-sectional area of the bed. As shown in Fig. 2, the minimum fluidization velocity is attained when the particles are fluidized. It is noteworthy that the velocity of inlet airflow is measured by the Testo 512 differential pressure meter. In the present study, the U_{mf} is obtained equal to 0.92 m/s, when the bed is filled by wet millet particles, and all experiments are carried out at an air velocity of 2.5U_{mf} which is equal to 2.3 m/s in order to ensure that all particles are fluidized in the bed.

2.3. Moisture ratio

The dry basis moisture is defined as the difference between the weights of the sample of grains and the fully dried grains and is given in Eq. (1) as follows [26,33]:

$$X_i = \frac{m_w - m_d}{m_d} \tag{1}$$

where X_i is the initial moisture, m_w represents the undried weight, and m_d is the dried weight. Regarding the constant moisture of the samples entering the bed, the X_i is obtained equal to 0.23 in all experiments.

The moisture content at any time is expressed in Eq. (2) as:

$$X = \frac{m_{wt} - m_{dt}}{m_{dt}} \tag{2}$$

where X is the moisture content at time t, m_{wt} is the weight of the millet sample exiting the bed at time t, and m_{dt} is the weight of the sample after being dried in the oven.

The most important experimental result is the moisture ratio which is calculated by Eq. (3) as follows:

$$MR = \frac{X - X_e}{X_i - X_e} \tag{3}$$

where MR, X, X_i and X_e are the moisture ratio, the moisture content on a dry basis, the initial moisture content on a dry basis, and the equilibrium moisture content on a dry basis, respectively. Given that over long drying times, the values of X_e become negligible compared to X_i, Eq. (3) is simplified into Eq. (4) during the drying process as [34]:

Table 2
Parameters of experiments.

Parameter	Value
Material	Foxtail millet
Diameter (m)	2.5 × 10^{-3}
Initial moisture (g of moisture/g of dry basis)	0.23
Drying temperature (°C)	40, 50, 60
Inlet flow pulse frequency (Hz)	0.5, 1, 2.5, continuous
Fluidization velocity (m/s)	2.3
Initial bed mass (g)	500
Initial height of particles in the bed (m)	0.05

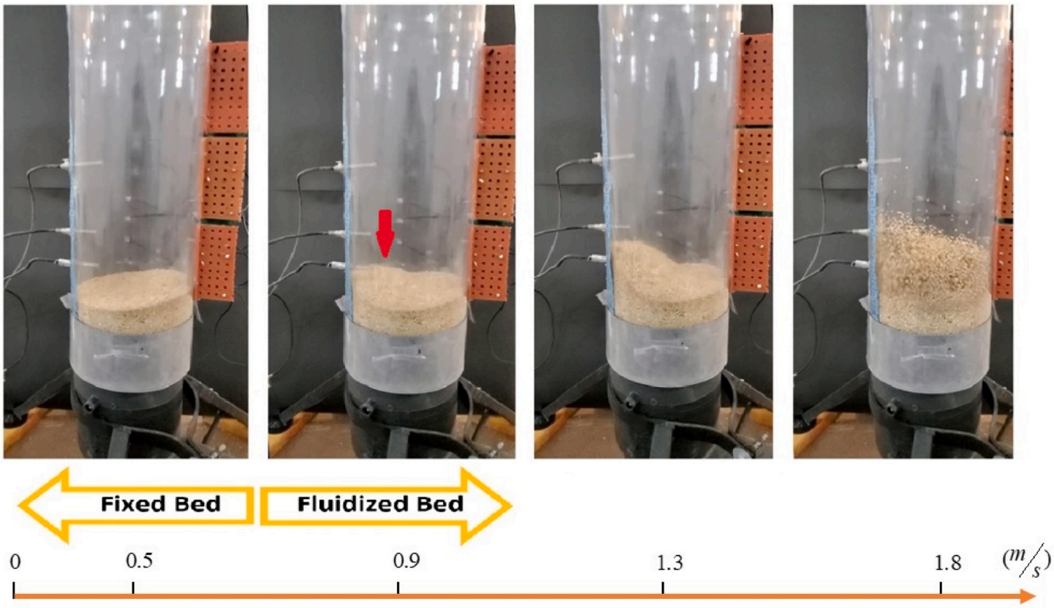

Fig. 2. Minimum flow fluidization velocity in continuous flow.

$$MR = \frac{X}{X_i} \tag{4}$$

2.4. *Error and uncertainty analysis*

An uncertainty analysis is performed on the experimental results to validate the measurements in the tests. Low measurement accuracy in empirical studies may occur due to inaccurate measurement devices and random changes in the operational conditions, calibration method, and data records. The uncertainty of any measurement can be expressed by the general relationship in Eq. (5) as follows [35]:

$$U_Y = \left[\left(\frac{\partial Y}{\partial z_1} u_1 \right)^2 + \left(\frac{\partial Y}{\partial z_2} u_2 \right)^2 + \ldots + \left(\frac{\partial Y}{\partial z_1} {u_n}^2 \right)^2 \right]^{\frac{1}{2}} \tag{5}$$

where U_Y is the uncertainty of the derived parameter of Y which is a function of the independent variables, z is the independent variable and u is the uncertainty of the independent variables. Various measuring instruments are used in experiments and the accuracy of the are listed in Table 3.

3. Results and discussion

3.1. *Hydrodynamic characteristics of the pulsed fluidized bed*

Fig. 3 shows the particle fluidization inside the bed for airflow with a frequency of 1 Hz before the valve opens and the sudden release of fluid for 1 s after the valve opens; in this case, the particles rise to a height of 0.35 m. The start and end of the process are shown on the left and right images, respectively.

Table 3
The accuracy of measuring instruments.

Parameter	Instrument	Accuracy
$T_{1\text{-}3}$	K-type Thermocouple	±0.5 °C
Mass	AND-EK-600G	±0.1 g
Velocity	Testo 512	±0.1 m/s
Flow meter	Ultrasonic Flow meter	±0.1 m^3/h
Diameter of the element	Caliper	±0.1 mm

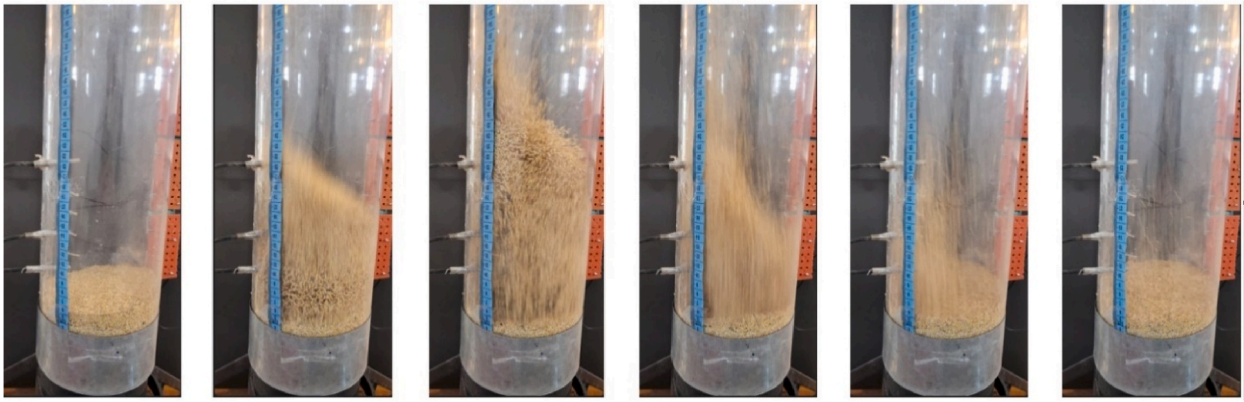

Fig. 3. Hydrodynamic behavior of pulsed fluidized bed at a frequency of 1 Hz and a velocity of 2.3 m/s.

3.2. Effect of the inlet fluid pulsation

The curves corresponding to moisture removal from the millet in the pulsed fluidized bed for different temperatures, different pulsation frequencies, and an average air velocity of 2.3 m/s are shown in Fig. 4 in terms of the *MR*-time graph. As seen in the figure, the *MR* continuously decreases as the drying time increases. A study of various *MR* graphs at different pulsation frequencies shows that there is an optimal flow frequency for this test and the effect of pulsation on drying is clearly observed. Moreover, it is determined that

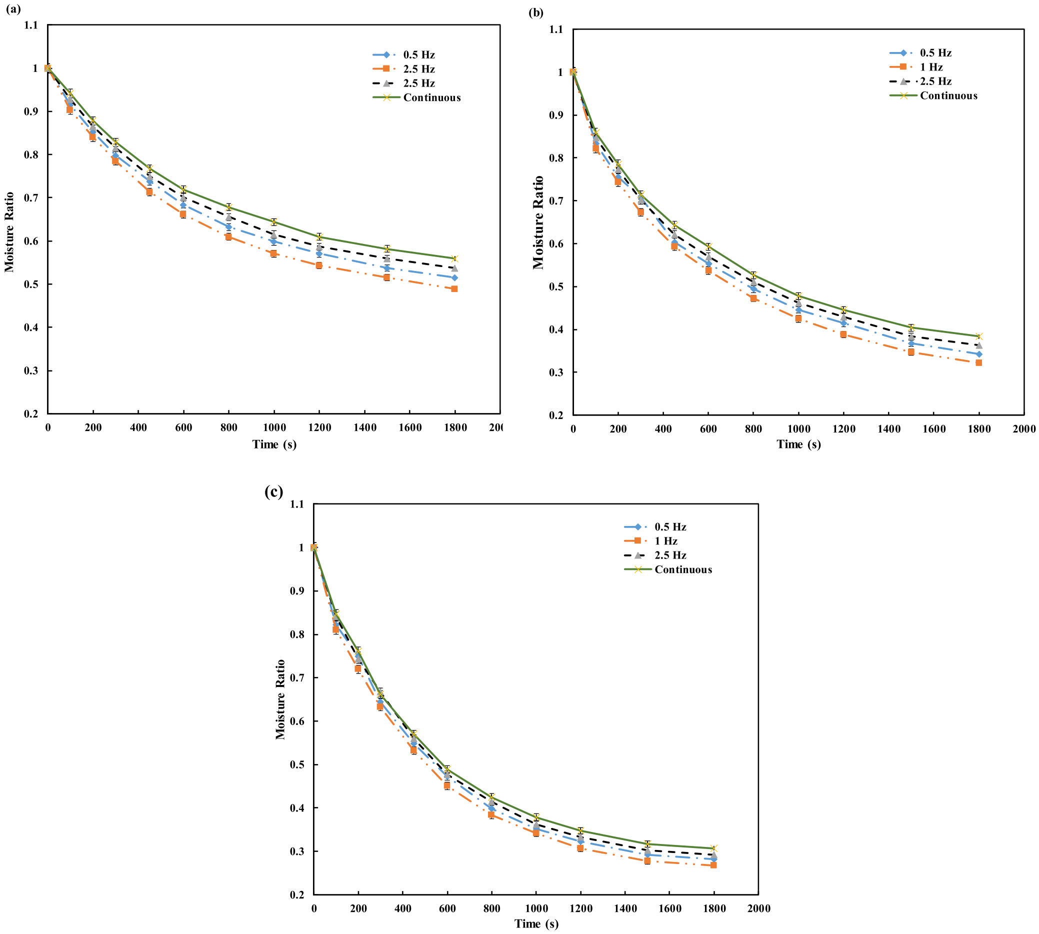

Fig. 4. Moisture ratio of millet drying in pulsed fluidized bed dryer as a function of time for different temperatures at $U = 2.3$ m/s, (a) 40 °C, (b) 50 °C, (c) 60 °C.

with an increase in the pulsation frequency of the inlet air from 0.5 to 1 Hz, the reduction rate of *MR* first increases with an increase in the upward particle circulation showing better mixing, the homogeneity in the bed, and further stability of the flow regime. However, the *MR* graph gradually approaches that of a continuous flow in a conventional fluidized bed as the pulsation frequency increases to 1 Hz and then to 5 Hz, making the flow regime approach that of a continuous flow. The best pulsation frequency for moisture removal is found to be at 1 Hz. In addition, regarding to the *MR* graphs in different flows with different temperatures, with a rise in the inlet air temperature, the pulsating flow still increases the moisture removal rate, but its effect decreases and the *MR* approaches that of a regular fluidized bed.

3.3. Effect of air temperature

Based on the *MR* graphs as shown in Fig. 4 for different pulsation frequencies and temperatures of airflow, the effect of a change in the frequency is different at different temperatures. Results in Fig. 4 demonstrate that the optimal frequency is equal to 1 Hz, thus the effect of inlet airflow temperature on the moisture ratio at the frequency of 1 Hz is illustrated in Fig. 5. From the obtained results, it can be found that not only there is an optimal frequency for moisture removal from millet grains but also there is an optimal temperature for moisture removal based on the comparison of the results at the end of the tests. For instance, at a fluid flow with a frequency of 1 Hz and temperature of 40 °C, the *MR* is 12.7 % lower than in the case of the conventional fluidized bed. This value is 15.5 % and 13 % at 50 °C and 60 °C. Furthermore, similar results are obtained at other times during the moisture removal process. Hence, the effect of changes in the pulsation frequency is different at different temperatures. It is found that the temperature of 50 °C has the greatest effect on pulsed flow compared to a conventional fluidized bed.

Results in Fig. 5 demonstrate that increasing the air temperature leads to faster moisture removal. As can be seen, the slope of the *MR* versus time graph becomes steeper as air temperature increases. This is caused by a rapid decrease in moisture on the grain surfaces due to the considerable amounts of heat from the higher air temperature and the faster moisture evaporation rate. In addition, the higher air temperature increases the activity of fluid molecules and reduces the density and viscosity, facilitating the diffusion of moisture from inside the grain to the grain surfaces [26]. For instance, with an increase in the temperature from 40 °C to 50 °C, a 9.5-min reduction in the drying time is required to reach a moisture content of 0.55. Moreover, an increase in the air temperature from 40 °C to 60 °C also leads to a 12-min decrease in this time.

3.4. Bed temperature

Fig. 6 shows the bed temperature for different pulsation frequencies during moisture removal from millet grains at an air velocity of 2.5 times of minimum velocity fluidization. The results indicate that the rise in the bed temperature occurs in two steps. The first step is shorter and involves a faster temperature rise, while the second step is longer and involves a slower temperature rise. The initial drying period is short. In this period, the temperature difference between the millet grains and the inlet air is the largest; hence, the bed temperature increases faster. Moreover, this period is sufficient for heating up the grains and initiating evaporation of the free moisture from their surfaces. Therefore, moisture removal occurs more rapidly in this period. This factor can also justify the higher moisture removal rate in the first period, mentioned in the previous section. After the end of the first step, the drying rate drop decreases for a longer period, indicating the internal mass transfer of the grains.

Comparing the results in Fig. 6 illustrates that during the moisture removal, an increase in the pulsation frequency from 0.5 to 1 Hz initially increases the bed temperature and drying at high rate. This can be attributed to the better mixing of the particles and the

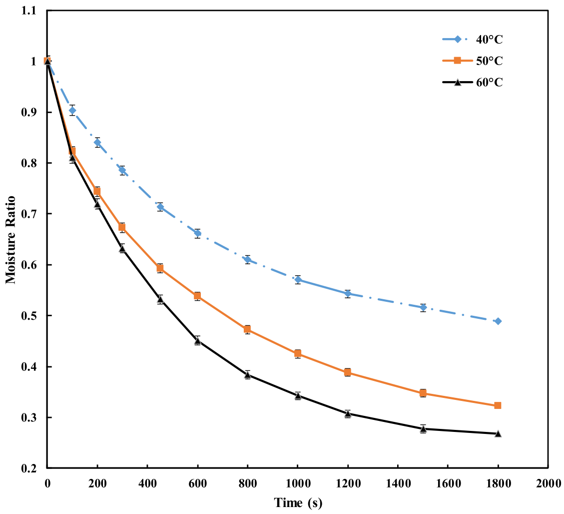

Fig. 5. Variations of moisture ratio at a frequency of 1 Hz for different air temperatures.

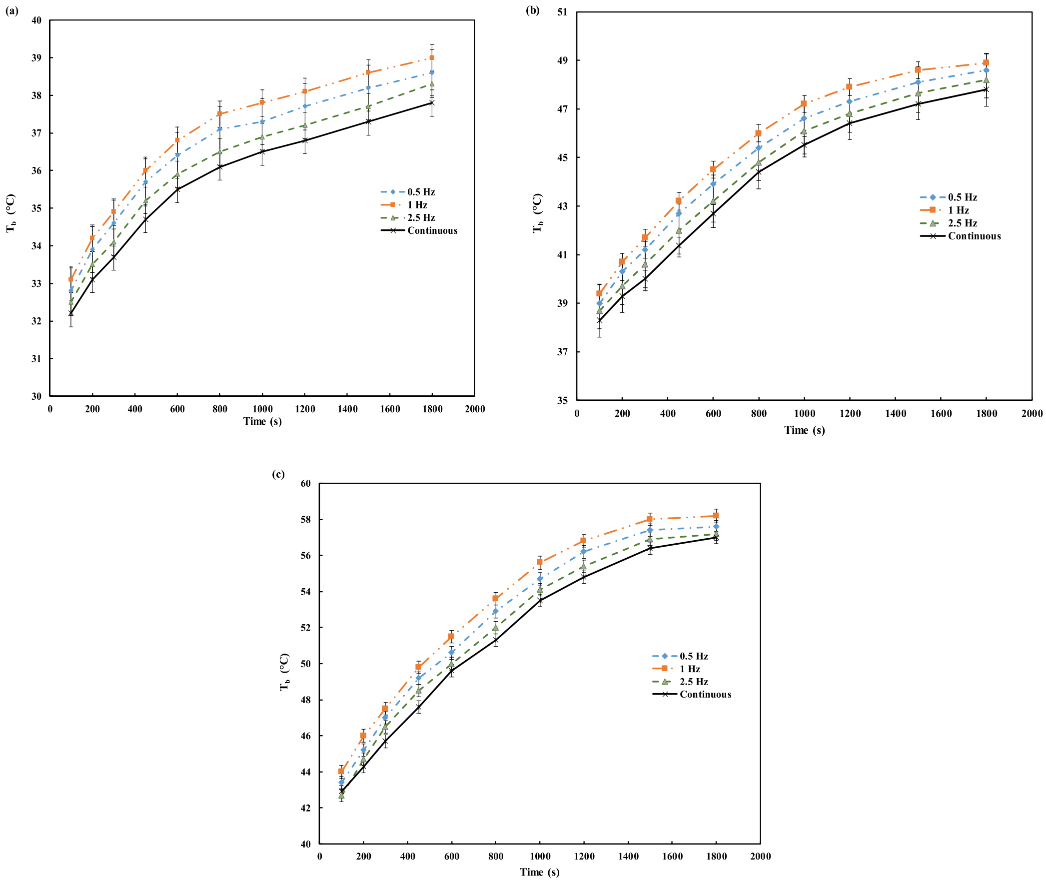

Fig. 6. Bed temperature as a function of time for different inlet air temperatures at $U = 2.3$ m/s, (a) 40 °C, (b) 50 °C, (c) 60 °C.

consequent increase in the particle air contact. With an increase in the inlet air pulsation frequency from 1 to 2.5 Hz, particle mixing decreases, because the flow behavior approaches that of a continuous flow. It is noteworthy that better particle air contact as compared to continuous flow is still witnessed in this case despite the reduction in particle mixing as compared to that with pulsation frequencies of 1 and 0.5 Hz. Thus, it can be concluded that the pulsation frequency of 1 Hz gives the best performance of pulsating fluidized bed.

To demonstrate the impact of the bed temperature, the moisture ratio as a function of bed temperature for different pulsation frequencies and inlet air temperature equal to 40, 50 and 60 °C at different drying times is illustrated in Fig. 7. Results indicate that the lower moisture ratio, the higher bed temperature at a specified drying time for all inlet air temperatures. For example at a drying time of 1000 min for a pulsation frequency of 1 Hz, moisture ratios are obtained equal to the bed temperature are 0.57, 0.42 and 0.34, and associated bed temperatures (T_b) are equal to 37.3, 46.6, 54.7 °C, at an inlet temperature of 40, 50 and 60 °C, respectively. Besides, by comparing the bed temperatures and moisture ratios at a constant pulsation frequency and inlet air temperature, it is found that the bed temperature increases as the drying time progresses, and consequently the moisture ratio decreases, which indicates more drying of foxtail millet grains. For instance, the bed temperature and associated moisture ratio are written in Table 4 for a pulsation frequency of 1 Hz and inlet air temperature of 50 °C. Results indicate that as the drying time progresses from 100 to 1800 min, the bed temperature is increased by 24.1 % and the moisture ratio is reduced by 60.7 %.

Overall, drying of solids is generally understood mostly to follow two distinct drying zones known as the constant rate period and falling rate period. The critical moisture content varies with the operating parameters and with the type of drying equipment. In this study using pulsating fluidized bed, the duration of constant rate period was found to be insignificant, considering the total duration of drying as shown in the figures. Similar results were reported using a multistage fluidized bed dryer staged externally, changing operating conditions experimentally by Yogendrasasidhar and Setty [36]. They reported drying characteristics of solids in dryers at various stages and comparison with single and multiple-stage fluidized bed dryers without noticing the two stages of drying.

3.5. Thin-layer semi-empirical model

As mentioned before, safe storage of food requires bringing it to a specific moisture level. To this end, it is necessary to examine the moisture absorption properties of a drying product. The development of a model for predicting the dependent variables of this process in terms of all the independent variables is a difficult task. Although numerous methods have been developed nowadays for predicting

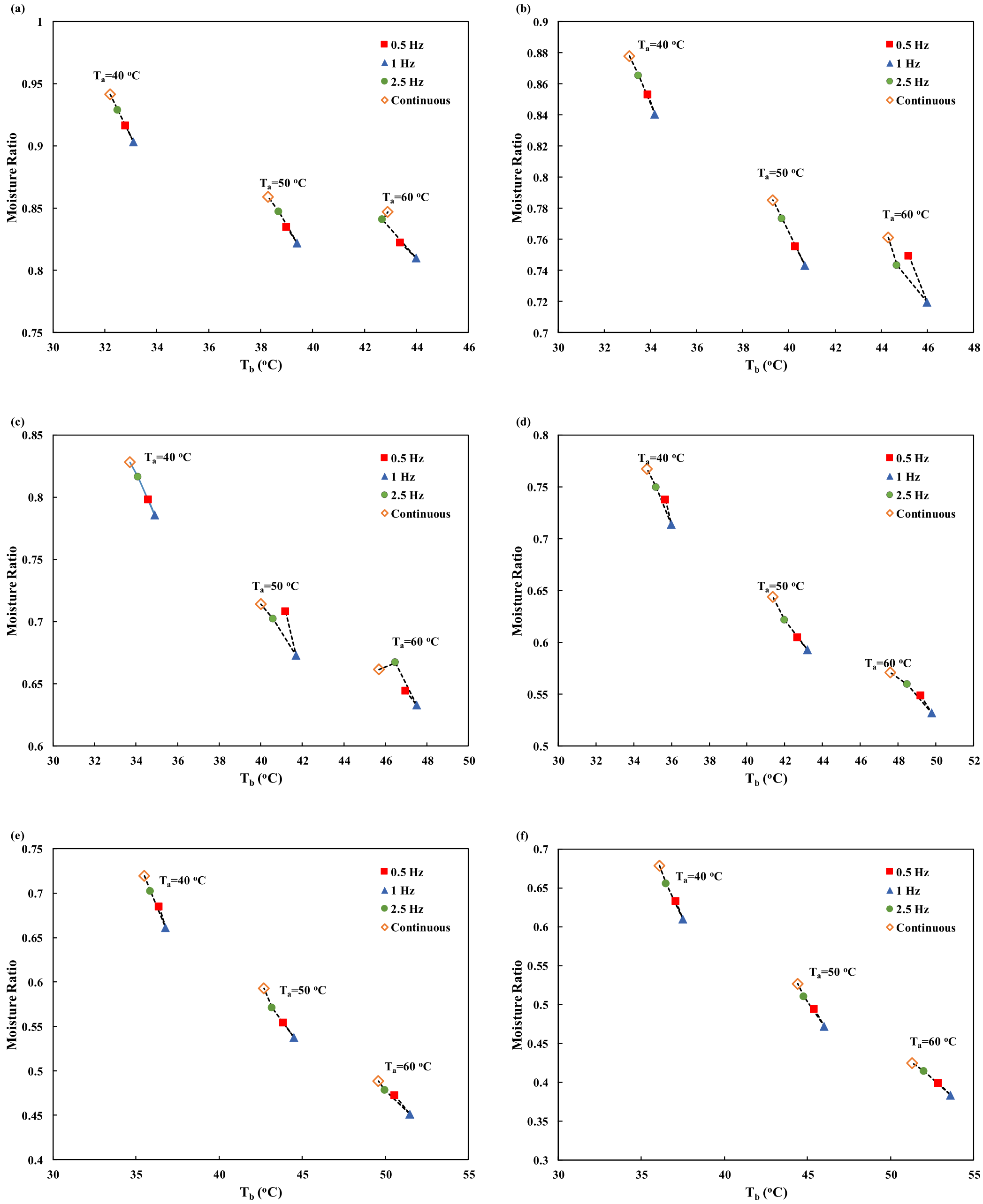

Fig. 7. Moisture ratio as a function of bed temperature for different pulsation frequencies, and inlet air temperature at a drying time of (a) 100 min, (b) 200 min, (c) 300 min, (d) 450 min, (e) 600 min, (f) 800 min, (g) 1000 min, (h) 1200 min, (i) 1500 min, and (j) 1800 min.

drying kinetics, most of these methods have low accuracy in predicting moisture drop during drying. Mathematical models have been widely used to predict the drying kinetics of several agricultural products, including soybeans [37], watermelon seeds [38] and papaya seeds [26].

The most common method for the prediction of moisture removal during the drying process is experimental or regression modeling. In this technique, different variables are measured in experimental tests, and the best algebraic relationships between the variables are selected based on the fitting of measured data to known drying kinetics algebraic equations. It is noted that product drying kinetics depends not only on the product type but also on the dryer type used to reduce moisture concentration. Hence, the drying kinetics is an important indicator for confirming the optimality of the process parameters [24]. Thin-layer mathematical models are proposed the fit a correlation over the experimental data [39]. These models describe heat and mass transfer during drying and mainly depend on the

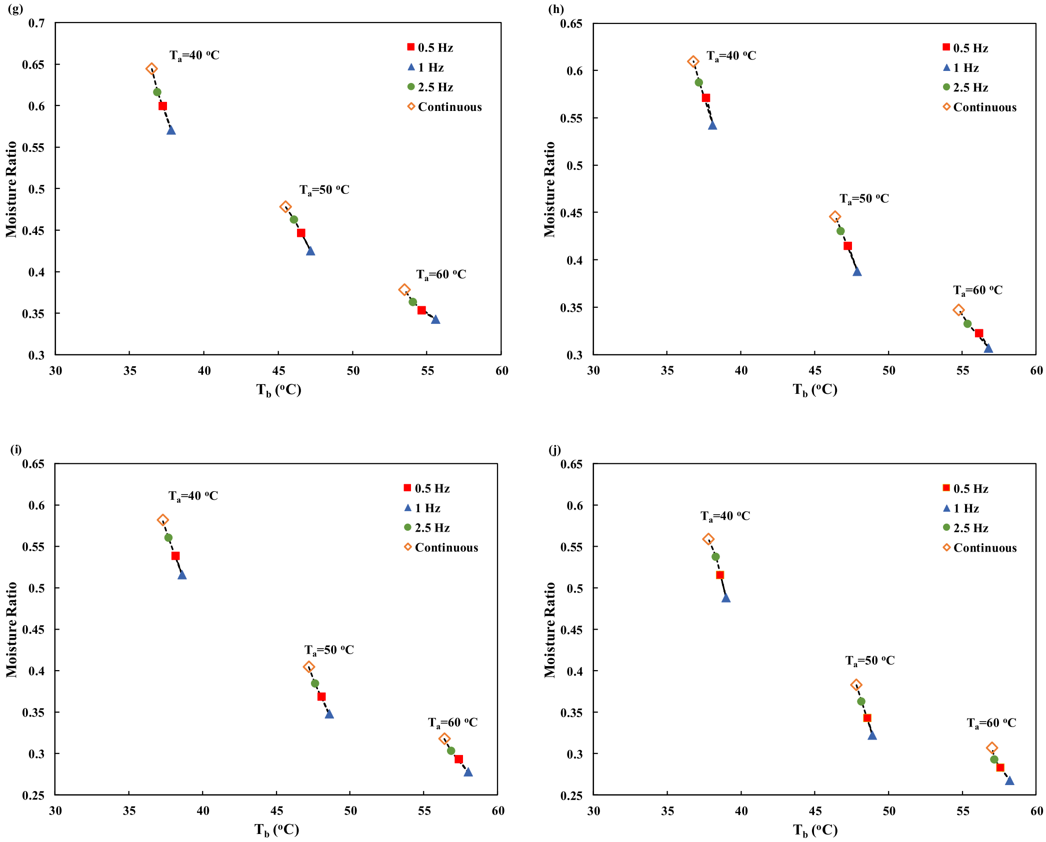

Fig. 7. (*continued*).

Table 4
Bed temperature and associated moisture ratio at different drying times for a pulsation frequency of 1 Hz and an inlet air temperature of 50 °C.

Drying time (min)	Bed temperature (°C)	Moisture ratio
100	39.4	0.82
200	40.7	0.74
300	41.7	0.67
450	43.2	0.59
600	44.5	0.53
800	46	0.47
1000	47.2	0.42
1200	47.9	0.38
1500	48.6	0.34
1800	48.9	0.32

material properties, drying parameters, and dryer type. Moreover, they clearly show the relationship between the process variables and the moisture removal process based on the drying time. These models have been considered for a wide range of drying conditions and material models. Since experimental models depend on measuring data, they facilitate the simulation of drying. However, these models cannot provide any information regarding the drying behavior of materials. In addition, they ignore the theoretical basis of

Table 5
Proposed models on drying kinetics.

Case	Moisture correlation
Midilli's model [40]	$\exp(-kt^n) + bt$
Page's model [40]	$\exp(-kt^n)$
Logarithmic model [40]	$a \times \exp(-kt) + c$
Approximation of Diffusion model [40]	$a \times \exp(-kt) + (1-a) \times \exp(-kbt)$

Table 6
Coefficients obtained for the correlations in different models for various pulsating frequencies and temperatures.

Frequency	Temperature (^oC)	Midilli's model [40]			Page's model [40]		Logarithmic [40]			Approximation of Diffusion [40]		
		k	*n*	*b*	*k*	*n*	*a*	*k*	*c*	*a*	*k*	*b*
0.5 Hz	40	0.002046	0.8589	0.0001337	0.006264	0.6315	0.5004	0.001609	0.4935	0.1026	1	0.0003661
	50	0.006464	0.7217	5.868e-05	0.01094	0.6186	0.6359	0.001841	0.3346	0.1623	1	0.0005882
	60	0.003516	0.8636	9.958e-05	0.01021	0.6611	0.7208	0.002115	0.2657	0.1604	1	0.0007991
1 Hz	40	0.002336	0.8489	0.0001309	0.007126	0.6246	0.5213	0.001682	0.4708	0.1129	1	0.0003952
	50	0.007688	0.7022	5.19e-05	0.01229	0.6106	0.6487	0.001925	0.3184	0.1748	1	0.0006222
	60	0.004586	0.8267	8.948e-05	0.01186	0.6457	0.7244	0.002214	0.2571	0.1764	1	0.0008242
2.5 Hz	40	0.001559	0.8969	0.0001488	0.005342	0.6449	0.4867	0.00156	0.5115	0.09141	1	0.0003478
	50	0.005672	0.7387	6.897e-05	0.01048	0.6182	0.622	0.001833	0.3525	0.156	1	0.0005602
	60	0.003065	0.8817	0.0001052	0.009394	0.6687	0.7169	0.002071	0.2734	0.1511	1	0.0007801
Continuous	40	0.001349	0.9088	0.0001502	0.004535	0.6572	0.4693	0.001491	0.5314	0.08093	1	0.0003255
	50	0.004781	0.7593	7.684e-05	0.009441	0.6253	0.6101	0.001761	0.367	0.1455	1	0.0005329
	60	0.002881	0.8889	0.0001136	0.009489	0.6618	0.7034	0.002086	0.2898	0.1501	1	0.0007444

drying, and their parameters are physically meaningless. Thus, they may describe drying behavior only under experimental conditions [27].

In order to model the drying kinetics of millet grains based on known mathematical models, the curve fitting tool of MATLAB software and the linear regression technique are applied to fit the experimental *MR* values to those predicted by four common models used to describe drying kinetics, presented in Table 5. Moreover, the constants, namely *k*, *a*, *b*, *c*, and *n* are written in Table 6, and the evaluation factors of the models are estimated.

In order to compare the performances of different models and the experimental moisture removal results, the corresponding equations are plotted in Fig. 8 for moisture removal at a temperature of 50 °C and a frequency of 2.5 Hz and in Fig. 9 for a continuous flow. As shown in Figs. 8 and 9, the model by Midilli's model [40] is the best among the fitted models, followed by the logarithmic model, then the page and approximation of diffusion are able to predict the experimental results.

The best model is selected via the nonlinear regression method. The parameters including the sum of squares of error (*SSE*) as stated in Eq. (6), the correlation coefficient (R^2) in Eq. (7), and the root mean squared error (*RMSE*) in Eq. (8) are considered to find the best correlation.

$$SSE = \frac{\sum_{i=1}^{N} \left(MR_{pre,i} - MR_{exp,i}\right)^2}{N} \tag{6}$$

$$R^2 = 1 - \left[\frac{\sum_{i=1}^{N} \left(MR_{pre,i} - MR_{exp,i}\right)^2}{\sum_{i=1}^{N} \left(MR_{exp,i} - \overline{MR}_{pre,i}\right)^2}\right] \tag{7}$$

$$RMSE = \left[\frac{1}{N} \sum_{i=1}^{N} \left(MR_{pre,i} - MR_{\exp,i}\right)^2\right]^{\frac{1}{2}} \tag{8}$$

where *SSE* is the sum of squares of error, *N* is the number of observations, $MR_{exp,i}$ is the *MR* observed in the ith measurement, and $MR_{pre,i}$ is the *MR* predicted from the ith measurement. In addition, R^2 is the correlation coefficient and *RMSE* is the root mean squared error. The *SSE*, R^2 and *RMSE* are calculated for both experimental data and results of predicted models. The higher R^2 and the lower SSE and *RMSE* represent a better model that estimates the drying curves. The values calculated for different testing conditions are presented in Table 7.

In general, the proposed models have comparable parameter values such as the maximum average R^2 in the range of 0.9624–0.9998, the minimum *SSE* from 0.186 to 0.0000953 and *RMSE* in the range of 0.0032–0.0474. Therefore, it is confirmed that these four models can be used to correctly predict the *MR* of millet grains with a temperature range of 40 °C–60 °C. Further analysis shows that the Midilli's model [40] is confirmed to be the most suitable model for predicting the moisture removal behavior of millet grains at drying temperatures of 40 °C, 50 °C, and 60 °C due to having the maximum average R^2 and minimum *SSE* and *RMSE*. The

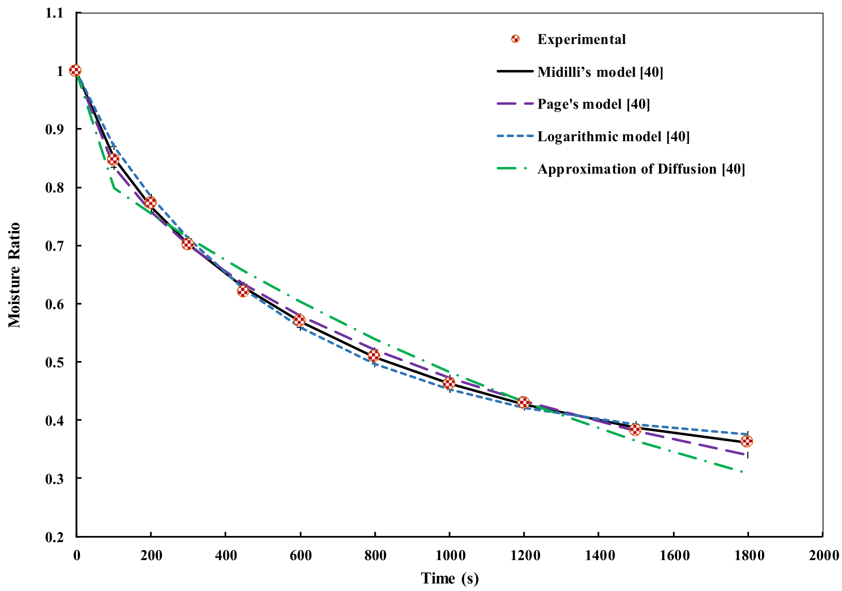

Fig. 8. Comparison of the experimental results with the drying models for a frequency of 2.5 Hz at a temperature of 50 °C and *U* of 2.3 m/s.

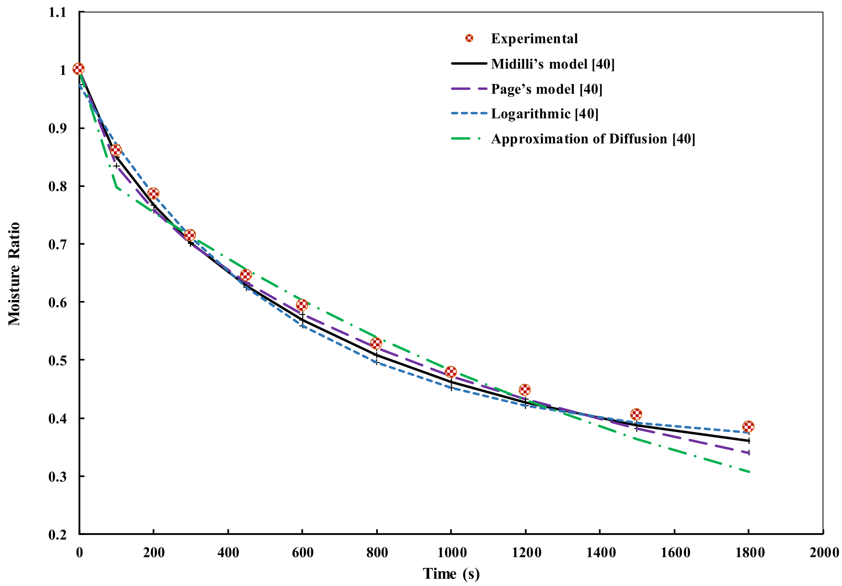

Fig. 9. Comparison of the experimental results with the drying models for a continuous flow at a temperature of 50 °C and *U* of 2.3.

performance of Midilli's model [40] along with a comparison of the experimental moisture (point) and the model (line) at different drying temperatures and a pulsation frequency of 1 Hz is shown in Fig. 10.

4. Conclusion

This research examined moisture removal from millet grains and determined the effect of pulsation frequency as a factor contributing to the drying of this product in a pulsed fluidized bed dryer. Different inlet flow conditions, namely pulsating flows with frequencies of 0.5, 1, and 2.5 Hz and a continuous flow at temperatures of 40 °C, 50 °C, and 60 °C were studied. Four semi-empirical thin-layer models common in drying kinetics were used to predict the drying kinetics of millet grains. It was determined that an increase in the pulsation frequency of the inlet air from 0.5 to 1 Hz improved particle mixing in the bed and increased the moisture ratio (*MR*) drop rate. With a further increase in the pulsation frequency from 2.5 to 5 Hz and as the flow regime approached a continuous flow, particle mixing decreased, and the bed began to resemble a conventional fluidized bed. A study of different *MR* graphs for pulsed flows of different frequencies and continuous flows indicated that there was an optimal frequency, which was determined to be 1 Hz for this study. Results demonstrated that increasing the drying temperature led to faster moisture removal. This was caused by a rapid decrease in moisture on the grain surfaces due to the considerable amounts of heat from the higher drying temperature for a faster moisture evaporation rate. Among the drying kinetics models, the predicted model which had a maximum average R^2 of 0.9994 and minimum SSE of 0.000246 and *RMSE* of 0.00525 was shown to be the most suitable model.

Funding

No funding was received.

Data availability statement

Data associated with this study has not been deposited into a publicly available repository. Nevertheless, data will be made available on request.

CRediT authorship contribution statement

Milad Setareh: Writing – review & editing, Supervision, Investigation, Formal analysis, Data curation, Conceptualization. **Mohammad Reza Assari:** Resources, Methodology, Conceptualization. **Hassan Basirat Tabrizi:** Writing – review & editing, Conceptualization. **Alireza Maghamian Zadeh:** Writing – original draft, Validation, Methodology, Formal analysis.

Declaration of competing interest

The authors declare that they have no known competing financial interests or personal relationships that could have appeared to influence the work reported in this paper.

Table 7
Statistical results of various drying models at different temperatures and pulsation frequencies.

Frequency	Temperature (°C)	Midilli's model [40]			Page 's model [40]			Logarithmic [40]			Approximation of Diffusion [40]		
		$SSE \times 10^{-4}$	R^2	$RMSE$	$SSE \times 10^{-4}$	R^2	$RMSE$	$SSE \times 10^{-4}$	R^2	$RMSE$	$SSE \times 10^{-4}$	R^2	$RMSE$
0.5 Hz	40	0.95317	0.9996	0.0035	24	0.9907	0.0165	1.6269	0.9994	0.0045	98	0.9624	0.0330
	50	4.8455	0.9989	0.0078	14	0.9969	0.0124	30	0.9933	0.0192	92	0.9792	0.0320
	60	6.5613	0.9989	0.0091	62	0.9893	0.0263	11	0.9981	0.0118	183	0.9684	0.0451
1 Hz	40	1.2125	0.9996	0.0039	27	0.9905	0.0174	2.3209	0.9992	0.0054	109	0.9621	0.0348
	50	0.81617	0.9998	0.0032	8.7350	0.9981	0.0099	34	0.9927	0.0205	89	0.9808	0.0315
	60	3.4180	0.9994	0.0065	50	0.9914	0.0237	13	0.9978	0.0126	173	0.9706	0.0439
2.5 Hz	40	1.2797	0.9995	0.0040	28	0.9885	0.0177	5.6144	0.9998	0.0026	99	0.9595	0.0332
	50	1.3493	0.9997	0.0041	13	0.9969	0.0121	22	0.9949	0.0164	97	0.9769	0.0329
	60	2.0116	0.9996	0.0050	62	0.9891	0.0263	4.7889	0.9992	0.0077	186	0.9674	0.0455
continuous	40	3.0412	0.9986	0.0062	0.0027	0.9880	0.0173	1.6449	0.9993	0.0045	0.0091	0.9594	0.0317
	50	1.0888	0.9997	0.0037	0.0015	0.9964	0.0127	17	0.9958	0.0145	0.0096	0.9761	0.0326
	60	2.9026	0.9995	0.0060	0.0069	0.9874	0.0277	3.8740	0.9993	0.0070	0.0202	0.9633	0.0474

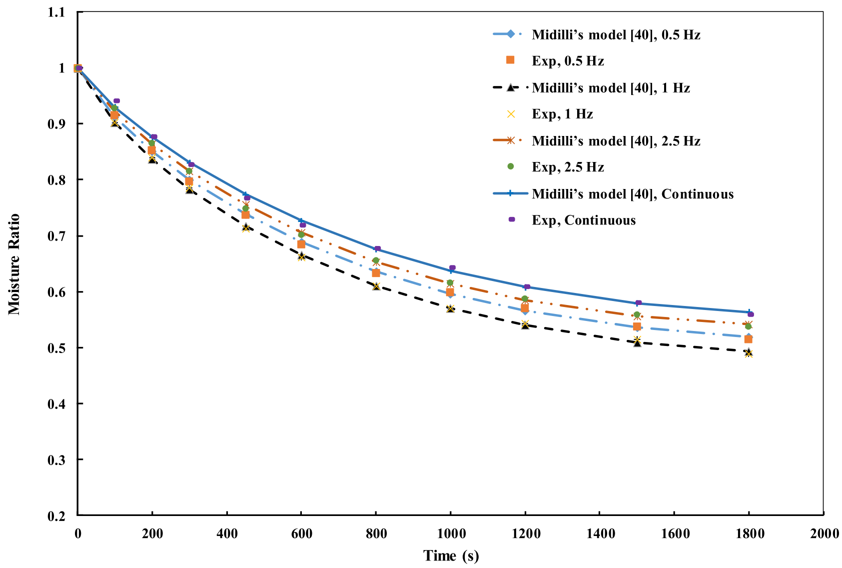

Fig. 10. Comparison between experimental and predicted drying model of millet in the pulsing fluidized bed, predicted data represented by lines (Midilli's model [40]).

References

[1] D. Chandra, S. Chandra, Pallavi, A.K. Sharma, Review of Finger millet (Eleusine coracana (L.) Gaertn): a power house of health benefiting nutrients, Food Sci. Hum. Wellness 5 (2016) 149–155, https://doi.org/10.1016/j.fshw.2016.05.004.

[2] R. Sehrawat, S. Abdullah, P. Khatri, L. Kumar, A. Kumar, A.S. Mujumdar, Role of drying technology in probiotic encapsulation and impact on food safety, Dry. Technol. 40 (2022) 1562–1581, https://doi.org/10.1080/07373937.2022.2044844.

[3] H.-W. Xiao, A.S. Mujumdar, Importance of drying in support of human welfare, Dry, Technol. 38 (2020) 1542–1543, https://doi.org/10.1080/07373937.2019.1686476.

[4] J. Azmir, Q. Hou, A. Yu, CFD-DEM study of the effects of food grain properties on drying and shrinkage in a fluidised bed, Powder Technol. 360 (2020) 33–42, https://doi.org/10.1016/j.powtec.2019.10.021.

[5] Z. Rezvani, H. Mortezapour, M. Ameri, H.-R. Akhavan, S. Arslan, Drying of Spirulina with a continuous infrared-assisted refractance window^{TM} dryer equipped with a photovoltaic-thermal solar collector, Heat Mass Tran. 58 (2022) 1739–1755, https://doi.org/10.1007/s00231-022-03210-5.

[6] G. Thamkaew, I. Sjöholm, F.G. Galindo, A review of drying methods for improving the quality of dried herbs, Crit. Rev. Food Sci. Nutr. 61 (2021) 1763–1786, https://doi.org/10.1080/10408398.2020.1765309.

[7] W. Abdesselem, M. Hemis, V. Raghavan, Experimental study of drying garlic slices (Allium sativum L.) using a fluidized-bed dryer, Heat Mass Transf. Und Stoffuebertragung 59 (2023) 229–237, https://doi.org/10.1007/S00231-022-03259-2/METRICS.

[8] S. Li, J. Qi, L. Wu, X. Wei, L. Yuan, H. Lin, Heat-fluid-solid coupling heat transfer analysis and parameter optimization in walnut drying device based on finite element method, Heliyon 10 (2024) e24931, https://doi.org/10.1016/j.heliyon.2024.e24931.

[9] S.B. Sasongko, H. Hadiyanto, M. Djaeni, A.M. Perdanianti, F.D. Utari, Effects of drying temperature and relative humidity on the quality of dried onion slice, Heliyon 6 (2020) e04338, https://doi.org/10.1016/j.heliyon.2020.e04338.

[10] J. Azmir, Q. Hou, A. Yu, Discrete particle simulation of food grain drying in a fluidised bed, Powder Technol. 323 (2018) 238–249, https://doi.org/10.1016/j.powtec.2017.10.019.

[11] D. Yogendrasasidhar, G. Srinivas, Y. Pydi Setty, Effect of distributor on performance of a continuous fluidized bed dryer, Heat Mass Transf. Und Stoffuebertragung 54 (2018) 641–649, https://doi.org/10.1007/S00231-017-2169-2/METRICS.

[12] M. Saidi, H. Basirat Tabrizi, S. Chaichi, M. Dehghani, The effect of non-continuous inlet air on increasing the segregation of binary particles in a fluidized bed, in: ASME Int. Mech. Eng. Congr. Expo. Proc., Mechanical Engineering Department, 424, Amirkabir University of Technology, Hafez Ave., Tehran, Iran, 2014, https://doi.org/10.1115/IMECE2014-37281.

[13] M. Nabipoor Hassankiadeh, M. Zarepour, L. Zhang, R.J. Spiteri, D. Bergstrom, Energy and exergy analysis of drying of potash particles in a pulsation-assisted fluidized bed, Int. J. Heat Mass Tran. 222 (2024) 125164, https://doi.org/10.1016/j.ijheatmasstransfer.2023.125164.

[14] H. Khosravi Bizhaem, H. Basirat Tabrizi, Investigating effect of pulsed flow on hydrodynamics of gas-solid fluidized bed using two-fluid model simulation and experiment, Powder Technol. 311 (2017) 328–340, https://doi.org/10.1016/j.powtec.2017.01.027.

[15] H.J. Das, P. Mahanta, R. Saikia, M.S. Aamir, Performance Evaluation of drying Ccharacteristics in conical bubbling fluidized bed dryer, Powder Technol. 374 (2020) 534–543, https://doi.org/10.1016/j.powtec.2020.06.051.

[16] M. Saidi, H. Basirat Tabrizi, G. Ahmadi, J.R. Grace, C.J. Lim, Hydrodynamics of pulsed spouted beds: effects of pulsation waveform, amplitude, and frequency, Dry. Technol. 34 (2016) 1546–1557, https://doi.org/10.1080/07373937.2015.1135942.

[17] K. Zhang, S. Wang, Y. Tang, Y. He, Prediction of segregation behavior of binary mixture in a pulsed fluidized bed, Adv. Powder Technol. 30 (2019) 2659–2665, https://doi.org/10.1016/J.APT.2019.08.013.

[18] P. Majumder, B. Deb, R. Gupta, S.S. Sablani, A comprehensive review of fluidized bed drying: sustainable design approaches, hydrodynamic and thermodynamic performance characteristics, and product quality, Sustain. Energy Technol. Assessments 53 (2022) 102643, https://doi.org/10.1016/j.seta.2022.102643.

[19] Y. Liu, H. Ohara, A. Tsutsumi, Pulsation-assisted fluidized bed for the fluidization of easily agglomerated particles with wide size distributions, Powder Technol. 316 (2017) 388–399, https://doi.org/10.1016/j.powtec.2016.12.049.

[20] M. Nabipoor Hassankiadeh, R.J. Spiteri, M. Berrey, D. Jordison, L. Zhang, D. Bergstrom, Wet fluidization characterization of potash particles in a pulsation-assisted fluidized bed, Powder Technol. 428 (2023) 118893, https://doi.org/10.1016/j.powtec.2023.118893.

[21] D. Jia, X. Bi, C.J. Lim, S. Sokhansanj, A. Tsutsumi, Biomass drying in a pulsed fluidized bed without inert bed particles, Fuel 186 (2016) 270–284, https://doi.org/10.1016/j.fuel.2016.08.100.

[22] P. Bengtsson, Experimental analysis of low-temperature bed drying of wooden biomass particles, Dry. Technol. 26 (2008) 602–610, https://doi.org/10.1080/07373930801946726.

[23] M. Khanali, A. Banisharif, S. Rafiee, Modeling of moisture diffusivity, activation energy and energy consumption in fluidized bed drying of rough rice, Heat Mass Tran. 52 (2016) 2541–2549, https://doi.org/10.1007/s00231-016-1763-z.
[24] M.H.T. Mondal, M. Akhtaruzzaman, M.S.H. Sarker, Modeling of dehydration and color degradation kinetics of maize grain for mixed flow dryer, J. Agric. Food Res. 9 (2022) 100359, https://doi.org/10.1016/j.jafr.2022.100359.
[25] M.J. Ortiz-Jerez, A.F. Sánchez, J.E. Zapata Montoya, Drying kinetics and sensory characteristics of dehydrated pumpkin seeds (Cucurbita moschata) obtained by refractance window drying, Heliyon 8 (2022) e10947, https://doi.org/10.1016/j.heliyon.2022.e10947.
[26] M. Alhanif, A.C. Kumoro, D.H. Wardhani, Thin-layer drying of papaya (Carica papaya) seeds: drying kinetics, mathematical modeling and effective moisture diffusivity, AIP Conf. Proc. 2610 (2022) 70007, https://doi.org/10.1063/5.0099562.
[27] A. Sozzi, M. Zambon, G. Mazza, D. Salvatori, Fluidized bed drying of blackberry wastes: drying kinetics, particle characterization and nutritional value of the obtained granular solids, Powder Technol. 385 (2021) 37–49, https://doi.org/10.1016/j.powtec.2021.02.058.
[28] Z. Li, M. van Sint Annaland, J.A.M. Kuipers, N.G. Deen, Effect of operating pressure on particle temperature distribution in a fluidized bed with heat production, Chem. Eng. Sci. 169 (2017) 299–309, https://doi.org/10.1016/j.ces.2016.04.046.
[29] M.R. Assari, M. Setareh, H. Basirat Tabrizi, A. Salehianfard, Experimental study on heat transfer and hydrodynamics of a concentric double-pipe pulsed fluidized bed using microencapsulated phase change material and sand, Powder Technol. 409 (2022) 117832, https://doi.org/10.1016/j.powtec.2022.117832.
[30] N. Sharma, K. Niranjan, Foxtail millet: properties, processing, health benefits, and uses, Food Rev. Int. 34 (2018) 329–363, https://doi.org/10.1080/87559129.2017.1290103.
[31] P.V.S. Patangare Suwarna S Syed HM and Shinde ST, Studies on physical properties and nutritional profile of foxtail millet, Pharma Innov. 8 (2019) 286–288.
[32] N. Hossain, R. Metcalfe, Performance analysis of a 2D numerical model in estimating minimum fluidization velocity for fluidized beds, Particuology 77 (2023) 116–127, https://doi.org/10.1016/J.PARTIC.2022.08.003.
[33] N.F. Beye, C. Kane, N. Ayessou, C.M.F. Kebe, C. Talla, C.M. Diop, A. Sène, Modelling the dehydration kinetics of four onion varieties in an oven and a solar greenhouse, Heliyon 5 (2019) e02430, https://doi.org/10.1016/j.heliyon.2019.e02430.
[34] Y. Xie, Y. Lin, X. Li, H. Yang, J. Han, C. Shang, A. Li, H. Xiao, F. Lu, Peanut drying: effects of various drying methods on drying kinetic models, physicochemical properties, germination characteristics, and microstructure, Inf. Process. Agric. (2022), https://doi.org/10.1016/j.inpa.2022.04.004.
[35] M. Setareh, M. Saffar-Avval, A. Abdullah, Heat transfer enhancement in an annulus under ultrasound field: a numerical and experimental study, Int. Commun. Heat Mass Tran. 114 (2020) 104560, https://doi.org/10.1016/J.ICHEATMASSTRANSFER.2020.104560.
[36] D. Yogendrasasidhar, Y.P. Setty, Experimental studies and thin layer modeling of pearl millet using continuous multistage fluidized bed dryer staged externally, Eng. Sci. Technol. an Int. J. 22 (2019) 428–438, https://doi.org/10.1016/j.jestch.2018.10.010.
[37] A. Anand, Y. Gareipy, V. Raghavan, Fluidized bed and microwave-assisted fluidized bed drying of seed grade soybean, Dry, Technol. 39 (2021) 507–527, https://doi.org/10.1080/07373937.2019.1709495.
[38] P. Dhurve, V. Kumar Arora, D. Kumar Yadav, S. Malakar, Drying kinetics, mass transfer parameters, and specific energy consumption analysis of watermelon seeds dried using the convective dryer, Mater. Today Proc. 59 (2022) 926–932, https://doi.org/10.1016/j.matpr.2022.02.008.
[39] Z. Tagnamas, M. Kouhila, Y. Bahammou, H. Lamsyehe, H. Moussaoui, A. Idlimam, A. Lamharrar, Drying kinetics and energy analysis of carob seeds (Ceratonia siliqua L.) convective solar drying, J. Therm. Anal. Calorim. 147 (2022) 2281–2291, https://doi.org/10.1007/s10973-021-10632-6.
[40] M. Hentabli, A.-E. Belhadj, H. Benimam, F. Dahmoune, S. Keskes, Vacuum drying of the Terbinafine HCl powder: a kinetics study and mathematical modeling, Powder Technol. 383 (2021) 220–232, https://doi.org/10.1016/j.powtec.2021.01.038.